

respectively (20). In the case of two-photon absorption, the line-shape function  $S(\nu)$  is proportional to  $1/[(\Omega - 2\nu)^2 + (\Gamma/2)^2]$  (21), where  $\Omega$  is the transition frequency,  $\nu$  is the laser frequency, and  $\Gamma$  is the molecular linewidth. Hence, to get  $\Gamma$ , the experimentally measured value  $\Delta\nu_0$  must be multiplied by a factor of 2. The molecular linewidth is more than twice the lifetime-limited value  $1/(2\pi T_1)$ . The difference may have been caused by spectral diffusion (22); further investigations are required to determine the origin of this difference. Spectral diffusion can also be responsible for fluctuations in the experimental values of  $\Delta\nu$  (Fig. 5).

From Eq. 8 and the experimental data, it follows that  $\sigma^{(2)} = 6 \times 10^{-45} \text{ cm}^4 \text{ s}$  (23). The parameters  $K$  and  $k_{31}$  can be estimated as well, because  $K = 2R_\infty T_{\text{rad}}/A_{\text{tot}}$  and  $k_{23} = 8 \times 10^5 \text{ s}^{-1}$  (24), giving  $K = 2.5 \times 10^{-2}$  and  $k_{31} = 1 \times 10^4 \text{ s}^{-1}$  (20). The value for  $k_{31}$  is in reasonable agreement with the triplet decay rate measured for shorter diphenylpolyenes [ $2.5 \times 10^3 \text{ s}^{-1}$  for diphenylhexatriene and  $4.1 \times 10^2 \text{ s}^{-1}$  for diphenylbutadiene (25)].

From our observations we conclude that the recorded signal corresponds to the emission of DPOT molecules excited by two photons. In spite of recent achievements in SM spectroscopy, it was not clear at the beginning of this research if the two-photon excitation of an SM was feasible at all. The extremely low cross section of two-photon absorption, thermal heating under excitation by strong laser light, and low count rate as a result of saturation were anticipated obstacles for such experiments. The very low background under two-photon excitation made our experiment possible.

## REFERENCES AND NOTES

- For reviews, see: W. M. Itano, J. C. Bergquist, D. J. Wineland, *Science* **237**, 612 (1987); H. Walther, *Aust. J. Phys.* **46**, 37 (1993), and references therein.
- E. Belzig and R. J. Chichester, *Science* **262**, 1422 (1993).
- Z. Hu and H. J. Kimble, *Opt. Lett.* **19**, 1888 (1994).
- W. E. Moerner and L. Kador, *Phys. Rev. Lett.* **62**, 2535 (1989).
- M. Orrit and J. Bernard, *ibid.* **65**, 2716 (1990).
- For the latest review, see: L. Kador, *Phys. Status Solidi B* **189**, 11 (1995).
- M. Göppert-Mayer, *Ann. Phys.* **9**, 273 (1931).
- R. M. Williams, D. W. Piston, W. W. Webb, *FASEB J.* **8**, 804 (1994); W. Denk, J. H. Strickler, W. W. Webb, *Science* **248**, 73 (1990).
- F. Güttler, Th. Iimgartinger, T. Plakhotnik, A. Renn, U. P. Wild, *Chem. Phys. Lett.* **217**, 393 (1994).
- W. P. Ambrose, P. M. Goodwin, J. C. Martin, R. A. Keller, *Science* **265**, 364 (1994).
- Chromophores of the octatetraene type have been thoroughly investigated [B. S. Hudson and B. E. Kohler, *J. Chem. Phys.* **59**, 4984 (1973); \_\_\_\_\_, K. Schulten, in *Excited States*, E. C. Lim, Ed. (Academic Press, New York, 1982), vol. 6, p. 1]. It was shown that the lowest singlet transition is of the  $2^1A_g \leftarrow 1^1A_g$  type. Two-photon excitation inhomogeneously broadened spectra of octatetraene in *n*-octane have been recorded [M. F. Granville, G. R.

- Holtom, B. E. Kohler, *J. Chem. Phys.* **72**, 467 (1980).
- H. Petek *et al.*, *J. Chem. Phys.* **98**, 3777 (1993).
- Cyclohexane solution, I. B. Berlman, *Handbook of Fluorescence Spectra of Aromatic Molecules* (Academic Press, New York, ed. 2, 1971).
- E. V. Shpol'skii, *Sov. Phys. Usp.* **6**, 411 (1963).
- T. Plakhotnik, W. E. Moerner, V. Palm, U. P. Wild, *Opt. Commun.* **114**, 83 (1995).
- The intensity of the inhomogeneous band varied by a factor of about 5 when the laser spot was moved from one place on the sample to another.
- W. E. Moerner and T. P. Carter, *Phys. Rev. Lett.* **59**, 2705 (1987).
- As no intensity redistribution between the zero-phonon line and the phonon wing was observed, interaction with phonons can cause only a dephasing. In this case thermal heating does not change the area of the zero-phonon line [K. K. Rebane, *Impurity Spectra of Solids* (Plenum, New York, 1970)].
- W. P. Ambrose, Th. Basché, W. E. Moerner, *J. Chem. Phys.* **95**, 7150 (1991); H. de Vries and D. A. Wiersma, *ibid.* **72**, 1851 (1979).

- On the basis of the measurement of a few molecules only, variations of the order of about 20% were observed in the low-power linewidth, the saturation intensity, and the high-power count rate. More statistics are needed to get the real distribution of these values.
- F. H. M. Faisal, *Theory of Multiphoton Processes* (Plenum, New York, 1987), p. 49.
- L. R. Narasimhan, D. W. Pack, M. D. Fayer, *Chem. Phys. Lett.* **152**, 287 (1988).
- The value is about four orders of magnitude larger than that measured at room temperature [R. J. M. Anderson, G. R. Holtom, W. M. McClain, *J. Chem. Phys.* **70**, 4310 (1979)] because of dramatic line narrowing at low temperature.
- R. Bensasson, E. J. Land, J. Lafferty, R. S. Sinclair, T. G. Truscott, *Chem. Phys. Lett.* **41**, 333 (1976).
- G. Heinrich, G. Holzer, H. Blume, D. Schulte-Frohlinde, *Z. Naturforsch. Teil B* **25**, 496 (1970).
- This work was supported by the Swiss National Science Foundation and by Eidgenössische Technische Hochschule Zurich.

30 October 1995; accepted 4 January 1996

## Are Single Molecular Wires Conducting?

L. A. Bumm, J. J. Arnold, M. T. Cygan, T. D. Dunbar, T. P. Burgin, L. Jones II, D. L. Allara,\* J. M. Tour,\* P. S. Weiss\*

Molecular wire candidates inserted into "nonconducting" *n*-dodecanethiol self-assembled monolayers on Au{111} were probed by scanning tunneling microscopy (STM) and microwave frequency alternating current STM at high tunnel junction impedance (100 gigohms) to assess their electrical properties. The inserted conjugated molecules, which were 4,4'-di(phenylene-ethynylene)benzenethiolate derivatives, formed single molecular wires that extended from the Au{111} substrate to about 7 angstroms above and had very high conductivity as compared with that of the alkanethiolate.

Molecular wires (MWs) are among the key components in the emerging field of molecular electronics. In their simplest form, MWs can be viewed as conjugated molecules that form one-dimensional electronic conductors to interconnect such proposed molecular devices as single electron transistors, electron turnstiles, molecular switches, and chemical sensors (1). Although many MW candidates have been prepared (2), the conductivity of single MWs has not been demonstrated. This is due in part to the difficulty of individually connecting a single MW to probes. In this report, we describe how molecular self-assembly was used both to anchor an MW candidate to an electrode (the Au{111} substrate) and to dilute and isolate the MW candidates within a self-assembled monolayer (SAM) of *n*-dodecanethiol (DT). The second connection

to the MW candidate was achieved via the probe tip of an STM or a tunable microwave frequency alternating current STM (ACSTM). The individual molecules can be observed in conventional STM images as well as by their microwave frequency electronic properties. The STM can then individually examine the inserted MW candidates and probe their electronic properties.

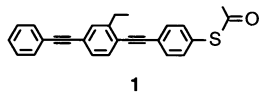
Bulk conductivity measurements of MW candidates include conduction paths along the molecule and percolation between the chains. Wu and Bein have grown isolated polyaniline molecules (3) and graphitic carbon (4) in zeolite matrices to eliminate interchain percolation and have demonstrated the molecules' conductivity using a microwave cavity perturbation technique at 2.63 GHz. Jones *et al.* (5) have made preliminary measurements using mechanical break junctions containing 1,4-benzenedithiol. Unfortunately, these tunnel junctions are ill defined in that it is difficult to know if the conducting channel is a single molecule or is even the molecule of interest. The STM and ACSTM are ideal for this study because they allow us to image the surface and locate isolated molecules, which are

L. A. Bumm, J. J. Arnold, M. T. Cygan, T. D. Dunbar, P. S. Weiss, Department of Chemistry, Pennsylvania State University, University Park, PA 16802, USA.  
T. P. Burgin, L. Jones II, J. M. Tour, Department of Chemistry and Biochemistry, University of South Carolina, Columbia, SC 29208, USA.  
D. L. Allara, Departments of Chemistry and Materials Science, Pennsylvania State University, University Park, PA 16802, USA.

\*To whom correspondence should be addressed.

then individually examined.

The MW candidate used was an ethyl-substituted 4,4'-di(phenylene-ethynylene)-benzothioacetate (**1**), which has been shown to self-assemble on Au when con-



verted to the thiolate (**1'** in Fig. 1) (6). The calculated length of **1'**, 21.3 Å (7), is 7.3 Å longer than the thickness of the DT monolayer on Au{111} (8), so that when coadsorbed it is expected to protrude beyond the methyl-terminated surface (Fig. 1). Even if tilted at the 30° angle of the DT molecules, the **1'** molecules would still protrude 4.0 Å above the DT film. Molecular modeling indicates that the **1'** molecules do not fit well into the DT lattice because of spatial constraints and poor van der Waals overlap with the surrounding DT molecules.

The SAM was prepared on Au{111}, which had been vapor deposited onto freshly cleaved, heated muscovite mica. The Au substrate was exposed to a 1 mM solution of DT in ethanol for 18 hours to form a well-ordered monolayer (9). After thorough rinsing of the sample (10), it was exposed to a 0.3 mM solution of **1** in tetrahydrofuran under dry Ar for 30 min. A small amount of aqueous ammonia was added to hydrolyze the thioacetyl protecting group, generating the thiol in situ to adsorb as the thiolate (**1'**) on the surface (6) as shown schematically in Fig. 1. We do not expect voids at the structural domain boundaries (as shown in Fig. 1), but rather conformationally relaxed DT molecules filling those spaces (11). After being rinsed and dried (10), the samples were stored at room temperature until imaged; exposure to air was limited. These SAMs were characterized by ellipsometry and by reflectance infrared spectroscopy (12).

Previously, we have shown STM images of phase-segregated  $\omega$ -substituted alkanethiolate monolayers on Au{111} (9). Fur-

thermore, we can differentiate between n-alkanethiolates of different chain lengths with molecular resolution in mixed composition SAMs (13). Here we used the DT monolayer as a matrix to support and to dilute the candidate MWs. Tour *et al.* have shown that **1'** chemisorbs to Au{111}, forming close-packed SAMs with the long molecular axis aligned nearly normal to the surface (6). Cygan *et al.* have demonstrated that the **1'** adsorbs into an existing DT SAM at film defects, such as domain boundaries (12), where the DT molecules can be conformationally relaxed. In contrast to neat **1'** SAMs in which the molecules can be oriented normal to the Au{111}, the molecular orientation might vary due to being imbedded in the DT film and because of conformational relaxation of the surrounding DT molecules at structural domain boundaries.

The STM and microwave frequency ACSTM used in these experiments have been described elsewhere (14). We measured the high-frequency conductivity of the tunnel junction by adding microwave frequency components to the conventional dc bias. In order to simplify detection of the high-frequency tunnel current, we simultaneously applied two frequencies separated by 5 kHz. The component of the tunnel current at the difference frequency was then extracted with a phase-sensitive detector. That this nonlinear scheme truly measures a high-frequency property of the tunnel junction can be understood as an application of Miller's rule (15). Namely, the  $n^{\text{th}}$ -order susceptibility for difference frequency generation is proportional to the product of the first-order susceptibilities at the frequency of each input and output (16).

STM images of the DT and **1'** SAM are shown in Fig. 2. We believe that the (bright) topographic features protruding through the DT film are due to **1'** because these features were not observed in the DT films before exposure to the solution of **1**. We infer that these features are due to single **1'** molecules because of the following observations: (i) Images of these fea-

tures where the DT molecular lattice is resolved show that the single **1'** molecular features are imaged with exactly the same shape, size, and orientation, which is indicative of features that are much sharper than the STM tip (Fig. 2B). (ii) Larger features (which we assign to clusters of **1'**) are only observed at Au{111} step edges where the DT SAM is expected to be conformationally relaxed and the **1'** molecules would be more easily accommodated (Fig. 2A). (iii) The **1'** molecules are observed to be widely separated on the terraces (Fig. 2A) and tend to occur at DT structural domain boundaries (Fig. 2)—

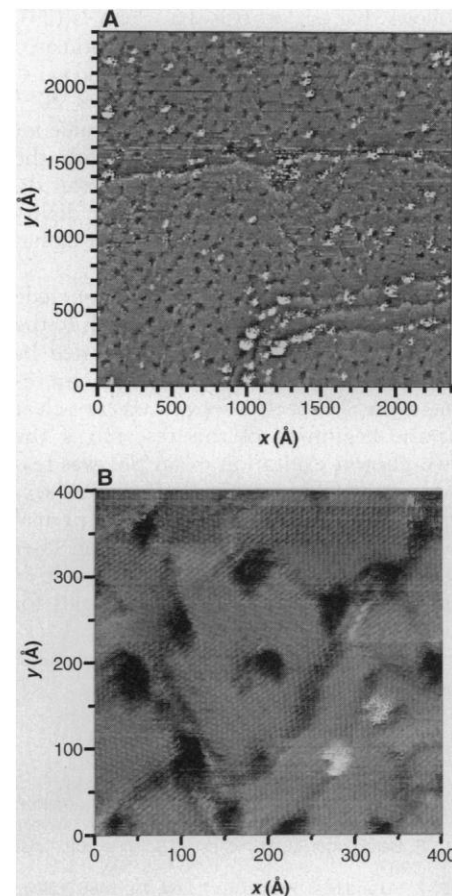
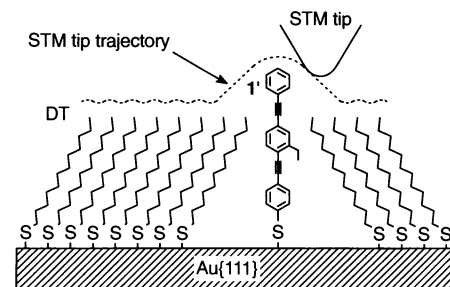


**Fig. 2.** Constant-current STM topographs of an Au{111} surface covered by DT and **1'** molecules (tip bias, 1.0 V; tunneling current, 10 pA). **(A)** A 2400 by 2400 Å image that has been displayed (by high-pass filtering) to show the distribution of **1'** molecules on several terraces simultaneously. The **1'** molecules on the Au terraces are widely separated and of uniform size, as opposed to the larger features at the Au step edges, which we assign as clusters of **1'** molecules. **(B)** An unprocessed 400 by 400 Å image showing DT molecular lattice resolution. Note the two **1'** molecules adsorbed at DT structural domain boundaries in the lower right quadrant of the image. The apparent shape of **1'** is a characteristic of this tip rather than of the molecule itself. These two **1'** molecules were observed to be stationary in the DT film for over 4 hours.

**Fig. 1.** A schematic representation of a DT and **1'** SAM on Au{111}. The height that the **1'** molecule extends above the DT film, if normal to the surface, is 7.3 Å. The trajectory of the STM tip traces out a surface of constant current. The relatively flat DT layer can be imaged by an atomic scale asperity on the end of the STM tip with resolution of the molecular lattice. The protruding **1'** molecule "images" the end of the STM tip, resulting in a characteristic feature due largely to the shape of the end of the STM tip for each **1'** molecule, as seen in subsequent figures. The STM tip is closer to the exposed ends of the **1'** molecules than to the exposed ends of the DT molecules because the ATBH is higher over the **1'** molecules than over the DT molecules.



only a small fraction of the DT structural domain boundaries on the Au{111} terraces are occupied by 1' features, which indicates that their insertion into the film is an isolated and improbable event. (iv) Direct insertion of clusters is unlikely because 1 is not known to be associated (in dimers and so on) in solution phase. The DT film forms domains of ( $\sqrt{3} \times \sqrt{3}$ ) R30° and related superstructures (17). Structural domain boundaries result from different alkyl chain tilt vectors and from sulfur-head-group-lattice registry. The dark features are due to the underlying Au substrate, which frequently develops pits that are a single atomic layer deep during exposure to alkanethiol solution (18). The 1' molecules were observed for as long as 4 hours and did not move or wander through the DT film. At the same time, the boundaries between the structural domains fluctuated as molecules at these interfaces changed their conformations.

STM topographic images are a convolution of the tip and surface geometry. When features on the surface are much sharper than the tip, such as the 1' single molecular protrusion about 7 Å higher than the DT film, each molecule is rendered as an image of the tip. This is shown schematically in Fig. 1 and can be seen in the images of 1' molecules (Fig. 2B), where each appears nearly identical in shape, size, and orientation. If more than a single 1' molecule were adjacent at the structural domain boundaries, each would contribute to the tunnel-

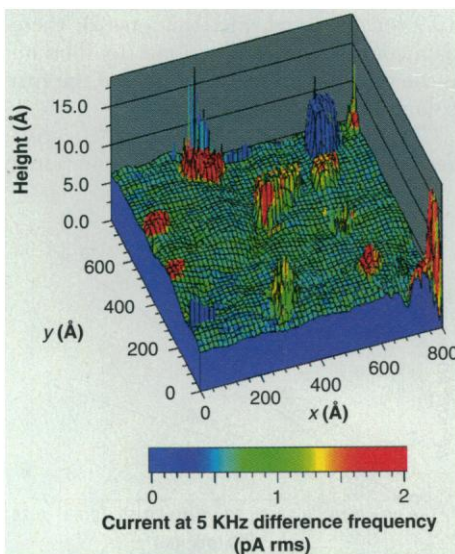


**Fig. 3.** A composite ACSTM image showing an 800 by 800 Å area of a Au{111} surface covered by DT and 1' molecules. The surface is derived from the constant-current topograph and the color is derived from the MDF signal (dc tip bias, 1.0 V; dc tunneling current, 10 pA; microwave frequencies, 5.0000000 GHz and 5.00000500 GHz applied to the ACSTM tip transmission line at about 1 mW each; detection at 5 kHz).

ing current. Thus the "tip image" from such a feature would be repeated and overlapped in a characteristic way. This is rarely found at the structural domain boundaries on terraces but is commonly found for the 1' molecules at substrate step edges. Most molecular resolution images are achieved on atomically flat surfaces, so that the sharpness of the tip is determined only by the endmost atomic scale asperity. Here, with the same tip, we do resolve the molecular lattice on the flat DT regions.

The apparent tunneling barrier height (ATBH) can be measured with the STM by modulation of the separation between the tip and sample ( $z$ ) and recording the derivative of the tunneling current ( $I$ ) with respect to this separation ( $dI/dz$ ) (19). The ATBH is at least two times higher over the 1' than over the DT. This higher relative ATBH, which is concurrent with greater tip-substrate separation (as shown schematically in Fig. 1), indicates that the junction contains regions of higher conductivity when the tip is over a 1' molecule than when it is over a DT molecule. Hence we infer that single 1' molecules have a higher conductivity than does the DT. We did not attempt to quantify the ATBH further because many factors come into play such as mechanical distortions of the tip and film. These complications make more than qualitative comparisons difficult at best (19, 20).

Figure 3 shows both the constant current STM topography (shown as surface topography) and the simultaneously acquired microwave difference frequency (MDF) ACSTM image (shown as surface color). Four types of features can be seen: (i) topographic maxima that coincide with MDF maxima, (ii) a single topographic maximum that does not coincide with the MDF maxima, (iii) MDF maxima that coincide with protrusions at DT film defects, and (iv) a Au{111} substrate atomic step.

The mechanism by which insulating molecules, such as DT monolayers, are imaged with the STM remains poorly understood (19). In contrast, the MW does have states that can be examined by STM. This is evident in the DC STM, the ATBH, and the ACSTM microwave difference frequency images.

The interpretation of STM topographic height differences is complicated because they are a function of the local density of states as well as the local barrier height (21). However, four observations lead us to infer that the 1' molecules are substantially more conducting than are DT molecules: (i) Unlike *n*-alkanethiolate films of similar thickness (that is, using 16-carbon-atom *n*-alkanethiols), the 1' molecules can be imaged nonperturbatively (22). (ii) The ATBH is higher over the 1' molecules despite their greater topograph-

ic height. (iii) We observe distinct contrast in the MDF images between the DT and the 1' molecules that is not observed for neat DT films or for SAMs of *n*-alkanethiols of mixed chain length. (iv) The differences in the topographic height in DC STM images between the DT and 1' molecules increase with decreasing junction impedance.

## REFERENCES AND NOTES

1. A. Aviram, Ed., *Molecular Electronics: Science and Technology* (Conference Proceedings No. 262, American Institute of Physics, New York, 1992); M. A. Reed and W. P. Kirk, Eds., *Nanostructure Physics and Fabrication* (Academic Press, New York, 1989); *Nanostructures and Mesoscopic Systems* (Academic Press, New York, 1992); F. L. Carter, Ed., *Molecular Electronic Devices II* (Dekker, New York, 1987); J. S. Miller, *Adv. Mater.* **2**, 378 (1990); *ibid.*, p. 495; *ibid.*, p. 601.
2. J. M. Tour, *Trends Polym. Sci.* **2**, 332 (1994).
3. C.-G. Wu and T. Bein, *Science* **264**, 1757 (1994).
4. ———, *ibid.* **266**, 1013 (1994).
5. L. Jones II *et al.*, *Polym. Prep.* **36**, 564 (1995).
6. J. M. Tour *et al.*, *J. Am. Chem. Soc.* **117**, 9529 (1995).
7. J. S. Schumm, D. L. Pearson, J. M. Tour, *Angew. Chem. Int. Ed. Engl.* **33**, 1360 (1994).
8. L. H. Dubois and R. G. Nuzzo, *Annu. Rev. Phys. Chem.* **43**, 437 (1992), and references therein.
9. S. J. Stranick, A. N. Parikh, Y.-T. Tao, D. L. Allara, P. S. Weiss, *J. Phys. Chem.* **98**, 7636 (1994).
10. The substrates treated with DT in ethanol were rinsed sequentially in hexane, acetone, and ethanol, and then blown dry in purified N<sub>2</sub>. The substrates further treated with 1 in tetrahydrofuran were rinsed sequentially in tetrahydrofuran, acetone, and ethanol, and then blown dry in purified N<sub>2</sub>. See (12) for the complete procedure.
11. S. J. Stranick, A. N. Parikh, D. L. Allara, P. S. Weiss, *J. Phys. Chem.* **98**, 11136 (1994).
12. M. T. Cygan *et al.*, in preparation.
13. L. A. Bumm *et al.*, in preparation.
14. S. J. Stranick and P. S. Weiss, *Rev. Sci. Instrum.* **64**, 1232 (1993); *ibid.* **65**, 918 (1994); L. A. Bumm and P. S. Weiss, *ibid.* **66**, 4140 (1995).
15. R. C. Miller, *Appl. Phys. Lett.* **5**, 17 (1964).
16. The exact mechanism of the microwave difference frequency contrast is not yet established. Possible mechanisms include heating (square law), difference frequency generation ( $\omega_{out}; \omega_1; \omega_2$ ), and modulated conductivity ( $\omega_{out}; 0; \omega_1; \omega_2$ ). Each of these mechanisms is linearly dependent on the power at each input frequency. Thus, we can measure the response of the tunnel junction at gigahertz frequencies by detecting a signal at 5 kHz.
17. G. E. Poirier and M. J. Tarlov, *Langmuir* **10**, 2853 (1994); G. E. Poirier, M. J. Tarlov, H. E. Rushmeier, *ibid.*, p. 3383.
18. J. A. M. Sondag-Huethorst, C. Schönenberger, L. G. J. Fokink, *J. Phys. Chem.* **98**, 6827 (1994).
19. See, for example, C. J. Chen, *Introduction to Scanning Tunneling Microscopy* (Oxford Univ. Press, New York, 1993).
20. V. Mujica, M. Kemp, M. A. Ratner, *J. Chem. Phys.* **101**, 6856 (1994).
21. N. D. Lang, *Phys. Rev. Lett.* **58**, 45 (1987); *Phys. Rev. B* **37**, 10395 (1988).
22. C. Schönenberger, J. Jorritsma, J. A. M. Sondag-Huethorst, L. G. J. Fokink, *J. Phys. Chem.* **99**, 3259 (1995).
23. We thank W. Ernst for the loan of a microwave source. The support of the Advanced Research Projects Agency; the NSF Chemistry, GRT, Materials Research, and PYI Programs; the Office of Naval Research; AT&T Bell Laboratories; the Biotechnology Research and Development Corporation, Eastman Kodak, Hewlett-Packard, IBM, and the Alfred P. Sloan Foundation is gratefully acknowledged.

28 September 1995; accepted 16 January 1996